PNAS
www.pnas.org

Supplementary Information for

Solvent selection criteria for temperature-resilient lithium-sulfur batteries

Guorui Cai, John Holoubek, Mingqian Li, Hongpeng Gao, Yijie Yin, Sicen Yu, Haodong Liu, Tod A. Pascal, Ping Liu, Zheng Chen*

*Corresponding author: Zheng Chen
Email: zhengchen@eng.ucsd.edu

This PDF file includes:

Figs. S1 to S23

Other supplementary information for this manuscript:

Movies S1 and S2

Fig. S1. Photos of selected electrolytes. Photos of 2 M LiFSI dissolved in G2, DME or DBE after storage at -60 ^{o}C overnight.

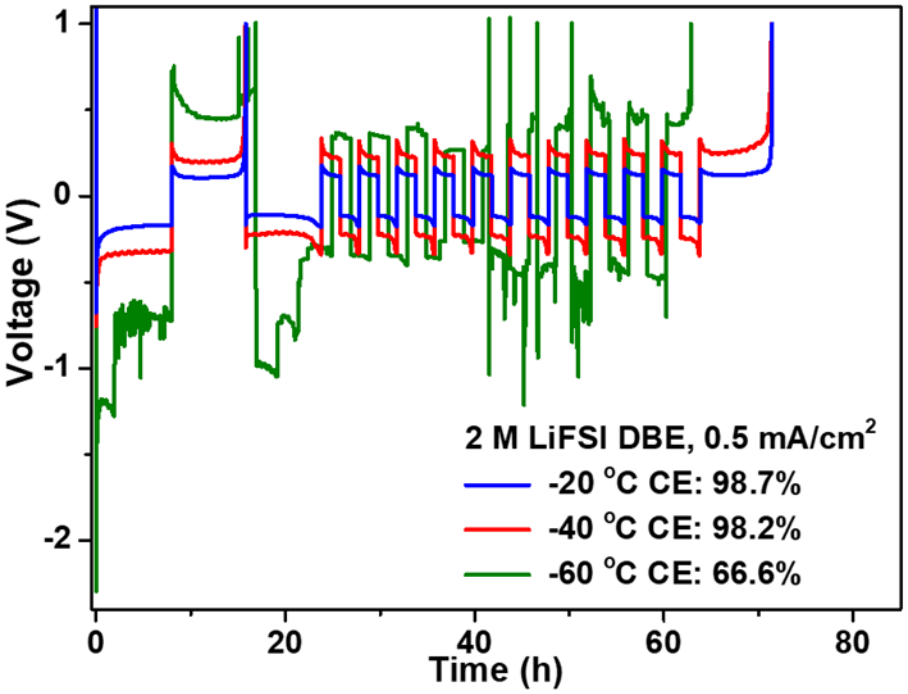

Fig. S2. CE determined curves for the electrolyte of 2 M LiFSI DBE at subzero temperatures.

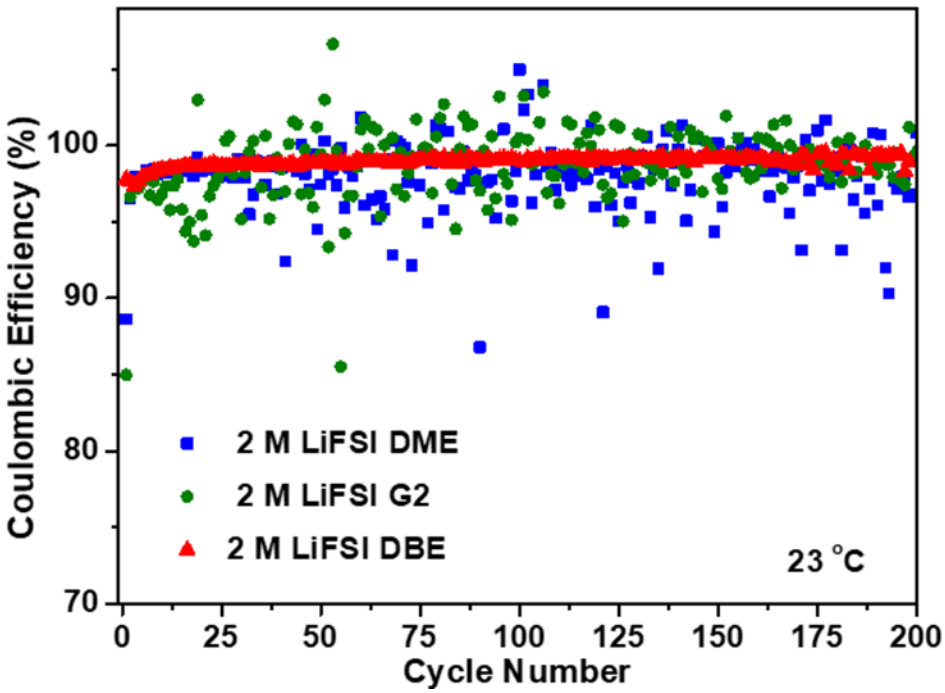

Fig. S3. Long-term cycling testing of Li//Cu cells in electrolytes of interest at 0.5 mA cm^{-2}, 1 mAh cm^{-2} and 23 ºC.

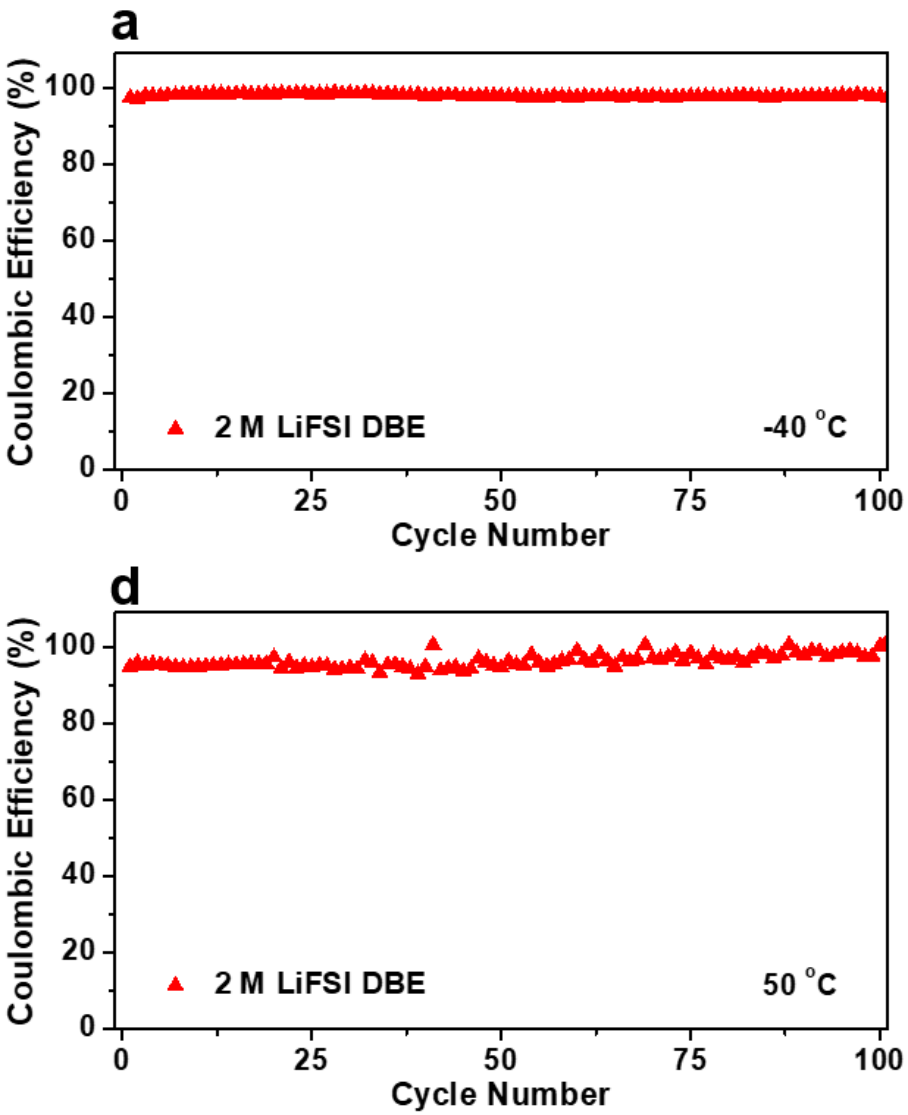

Fig. S4. Long-term cycling testing of Li//Cu cells in 2 M LiFSI DBE with 0.5 mA cm^{-2}, 1 mAh cm^{-2} at (a) -40 and (b) 50 ^{o}C.

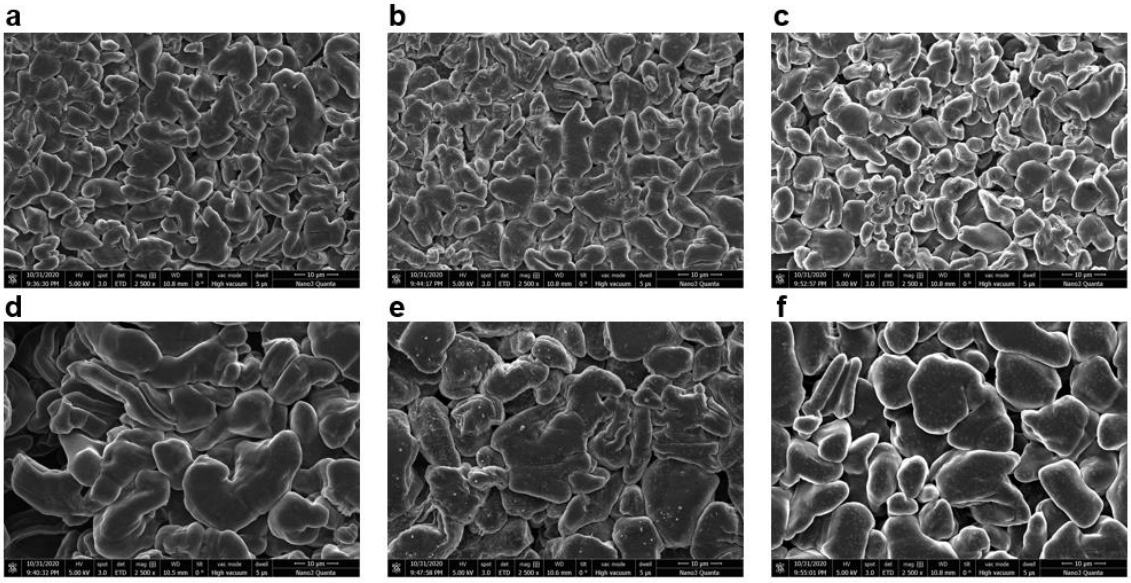

Fig. S5. The SEM images of plated Li metal at (a-c) 23 ^{o}C and (d-f) 50 ^{o}C in selected electrolytes: (a, d) 2 M LiFSI G2, (b, e) 2 M LiFSI DME, (c, f) 2 M LiFSI DBE.

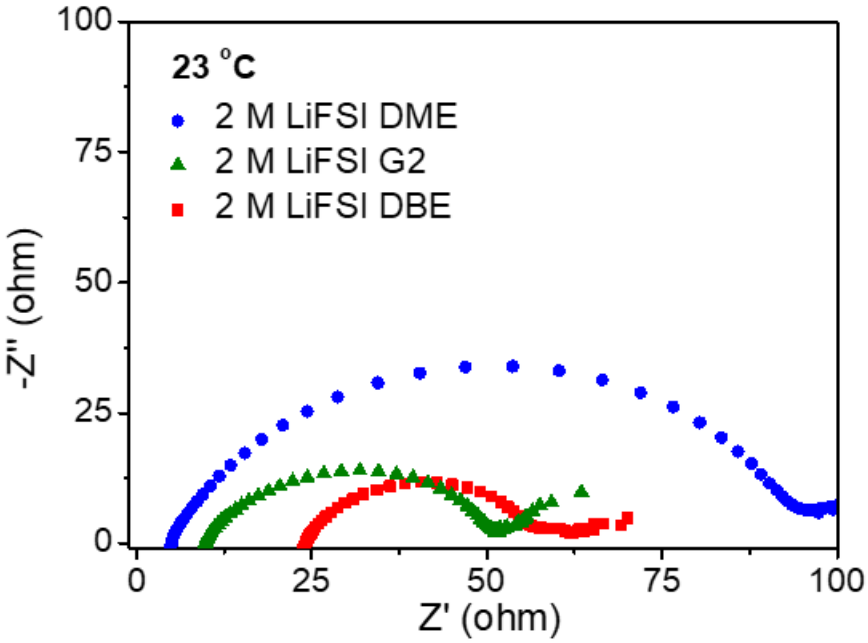

Fig. S6. EIS profiles of Li//Li symmetrical cells collected at 23 °C in selected electrolytes.

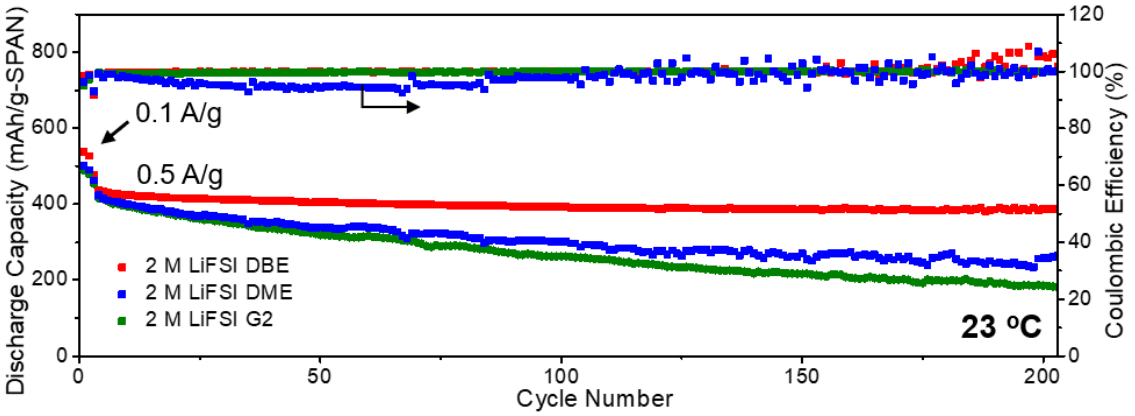

Fig. S7. Cycling performance of Li//SPAN half cells with a SPAN loading of ~1.0 mAh cm^{-2} in each electrolyte at 23 °C and 0.5 A g^{-1}.

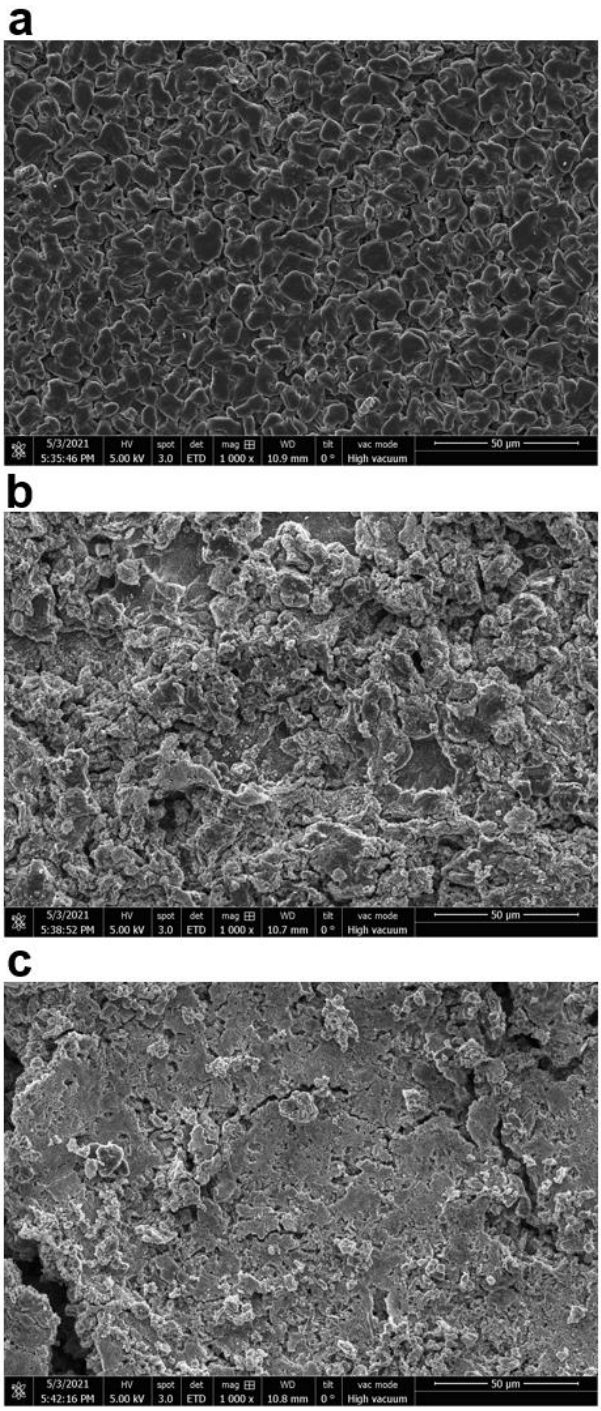

Fig. S8. SEM images of cycled Li metal in (a) 2 M LiFSI DBE, (b) 2 M LiFSI DME, and (c) 2 M LiFSI G2, obtained by disassembling the Li//SPAN half cells after 10 cycles at 50 ºC.

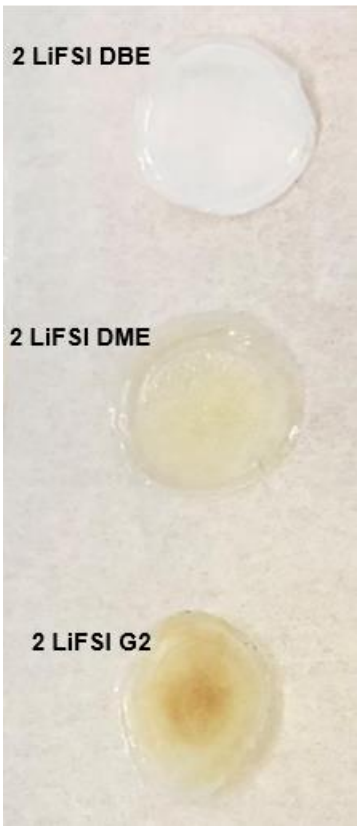

Fig. S9. Digital photographs of separators obtained by disassembling the Li//SPAN cells with selected electrolytes after cycling at 50 ºC for 10 cycles. The obtained separators were dried in Ar-filled glovebox overnight before collecting the optical photographs.

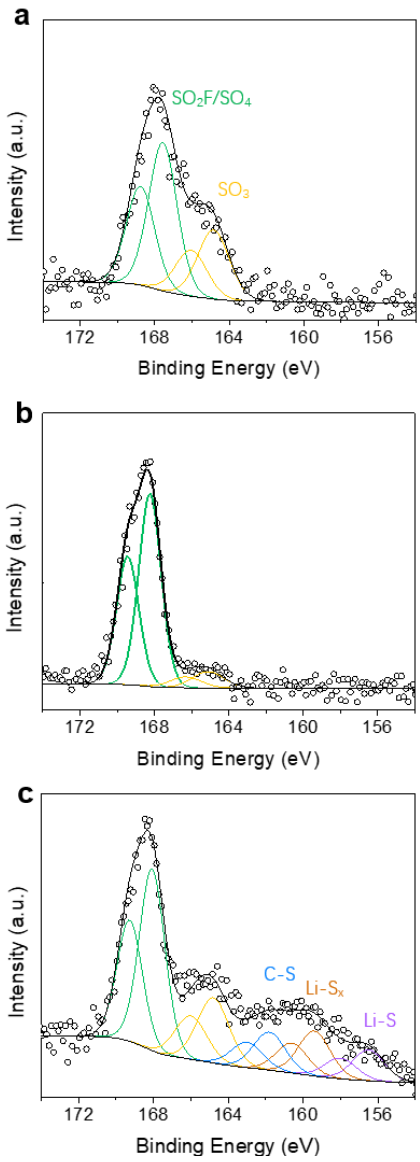

Fig. S10. X-ray photoelectron spectroscopy (XPS) spectra of delithiated SPAN cathodes obtained by disassembling the Li//SPAN cells with selected electrolytes after cycling at 50 °C for 10 cycles: (a) 2 M LiFSI DBE, (b) 2 M LiFSI DME, (c) 2 M LiFSI G2.

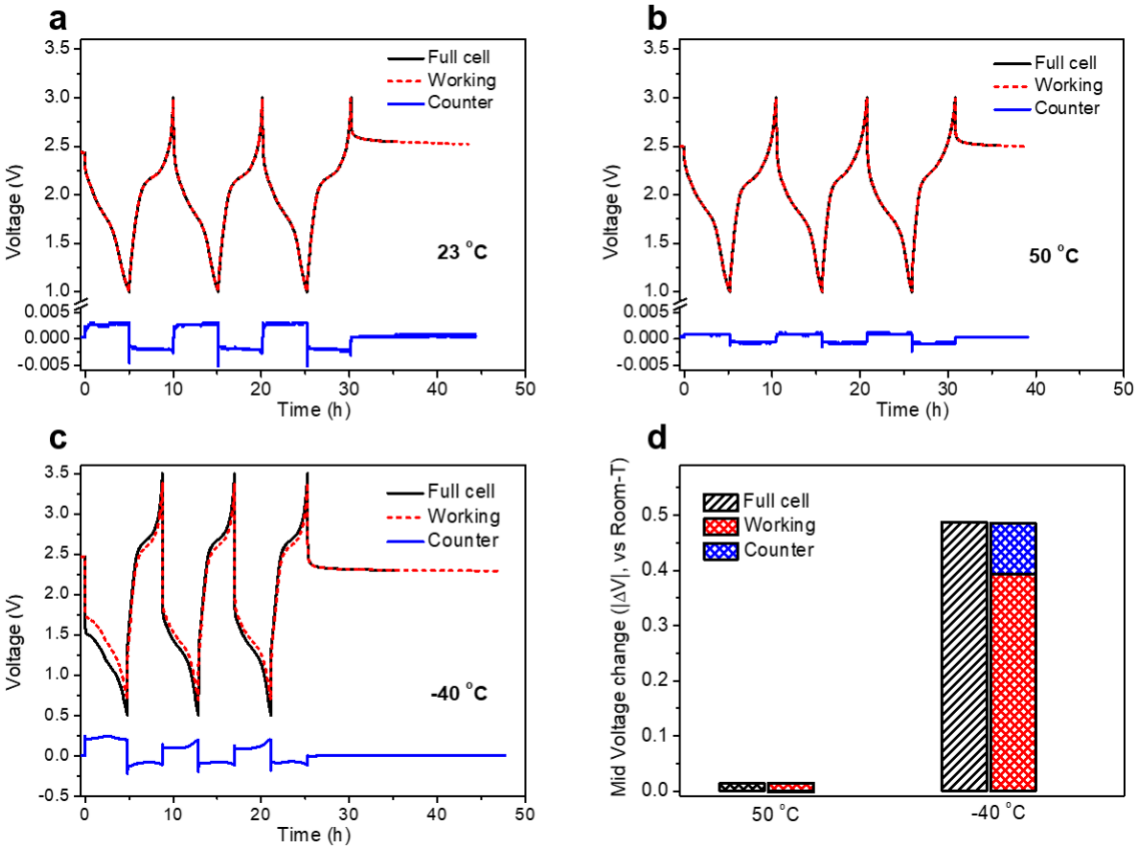

Fig. S11. Voltage-time curves of Li||Li||Cu three-electrode cells with 0.1 A g^{-1} and 2 M LiFSI DBE at (a) 23 °C, (b) 50 °C, (c) -40 °C, in which Li disc as the counter electrode, SPAN cathodes as the working electrodes, and a small Li attached on copper wires as the reference electrodes. (d) The middle value changes (absolute value) in discharging curves at 50 °C and -40 °C compared with the value at 23 °C.

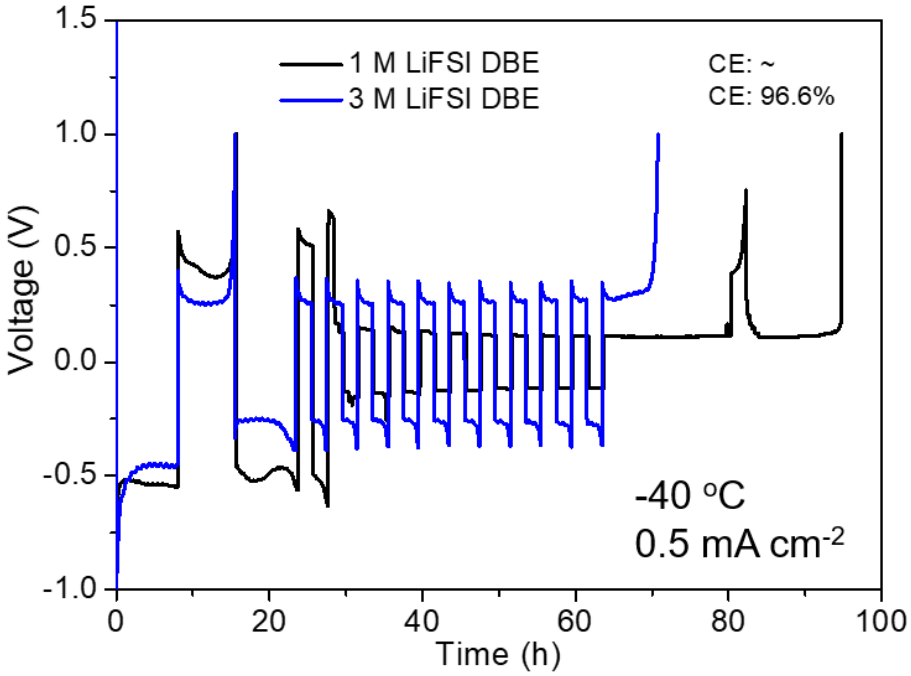

Fig. S12. CE determined curves for the electrolytes of 1 M and 3 M LiFSI in DBE at -40 °C. The CE for 1 M LiFSI DBE is failed to be obtained due to a soft-shorting event.

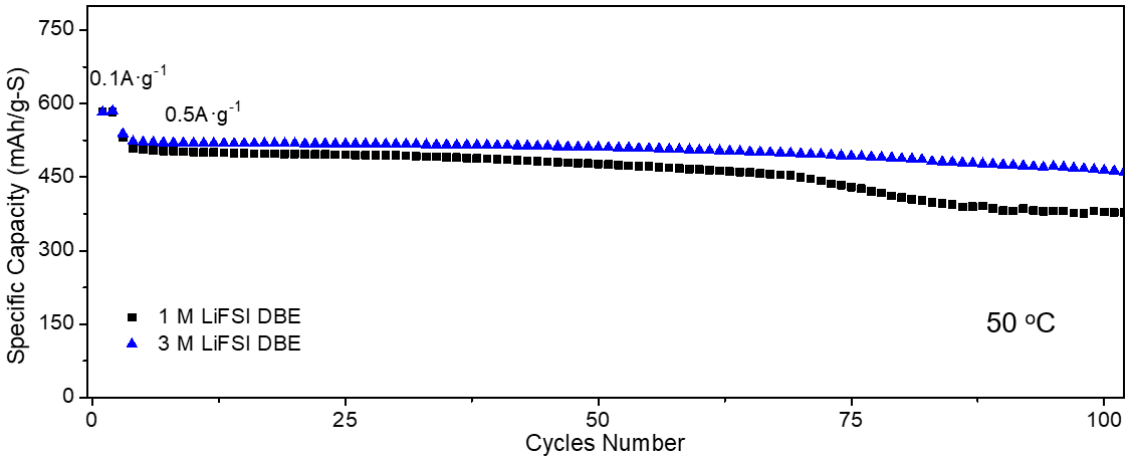

Fig. S13. Cycling performance of Li//SPAN half cells in each electrolyte at 50 °C and 0.5 A g^{-1}.

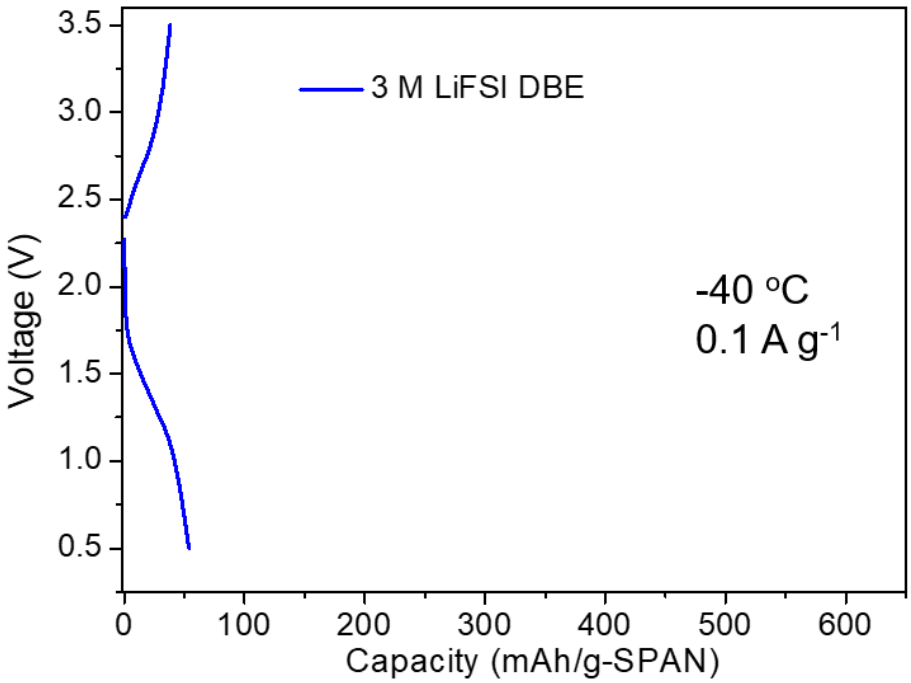

Fig. S14. Voltage-capacity curves of Li//SPAN half cells in 3 M LiFSI DBE at -40 °C with a current density of 0.1 A g^{-1}.

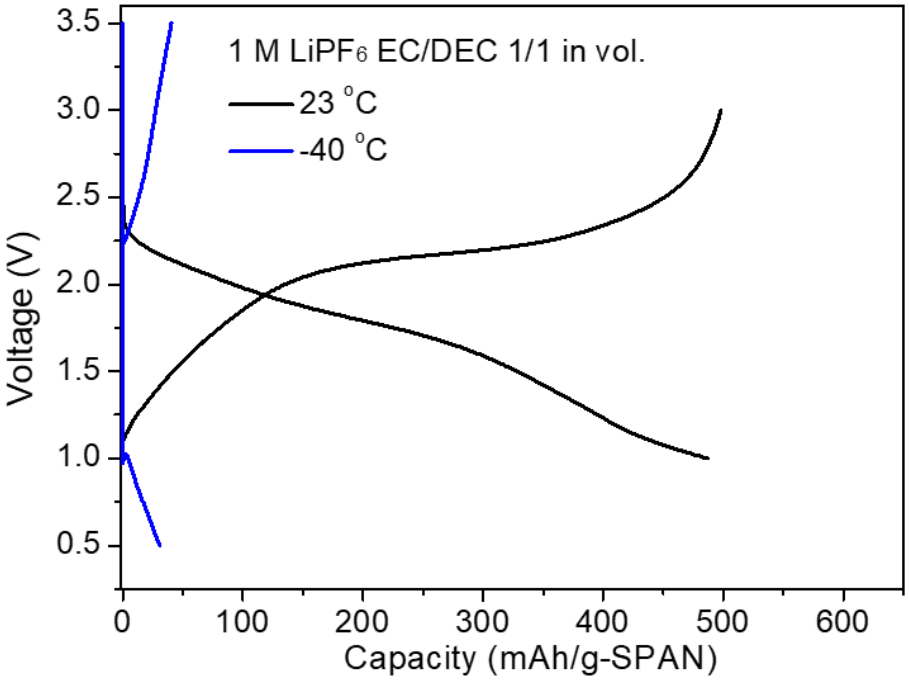

Fig. S15. Voltage-capacity curves of Li//SPAN half cells in 1 M $LiPF_6$ EC/DEC 1/1 in vol. at 23 and -40 ^oC with a current density of 0.1 A g^{-1}.

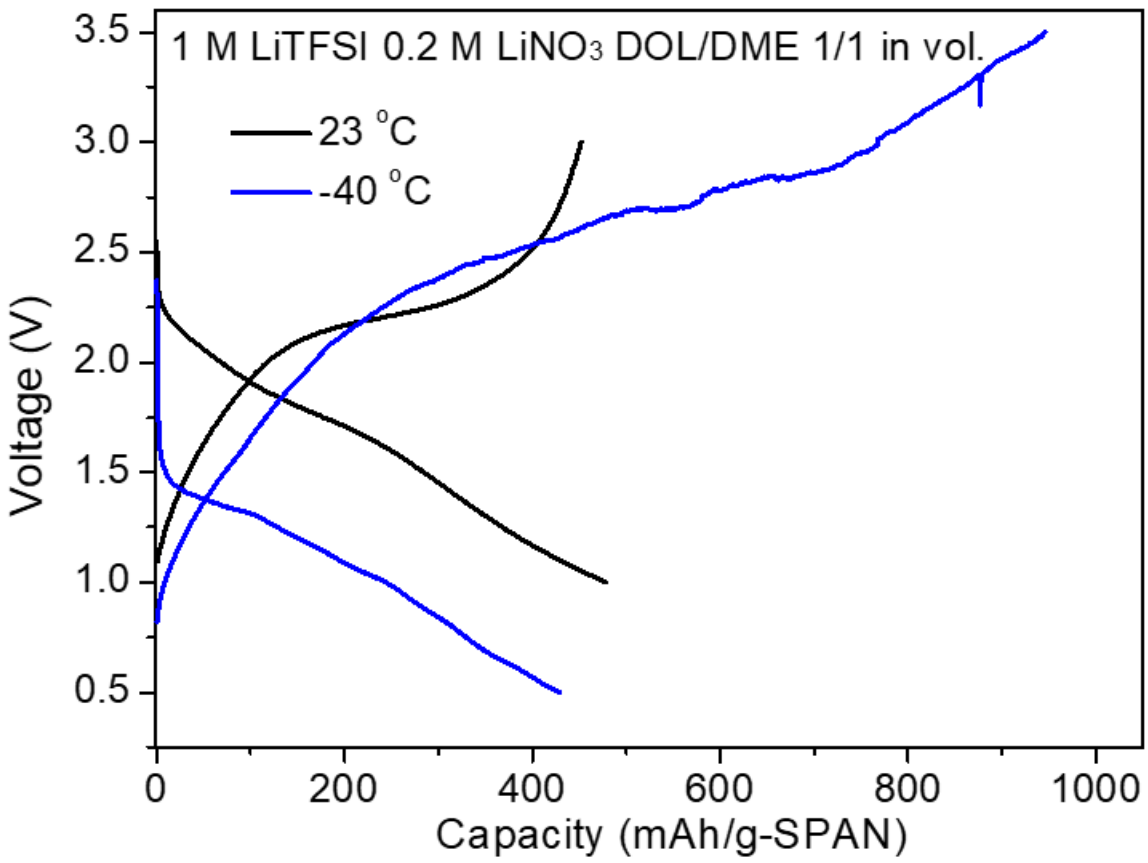

Fig. S16. Voltage-capacity curves of Li//SPAN half cells in 1 M LiTFSI 0.2 M $LiNO_3$ DOL/DME 1/1 in vol. at 23 and -40 ºC with a current density of 0.1 A g^{-1}. The fluctuated charging curve can be attributed to the soft-shorting during Li metal plating at subzero temperatures.

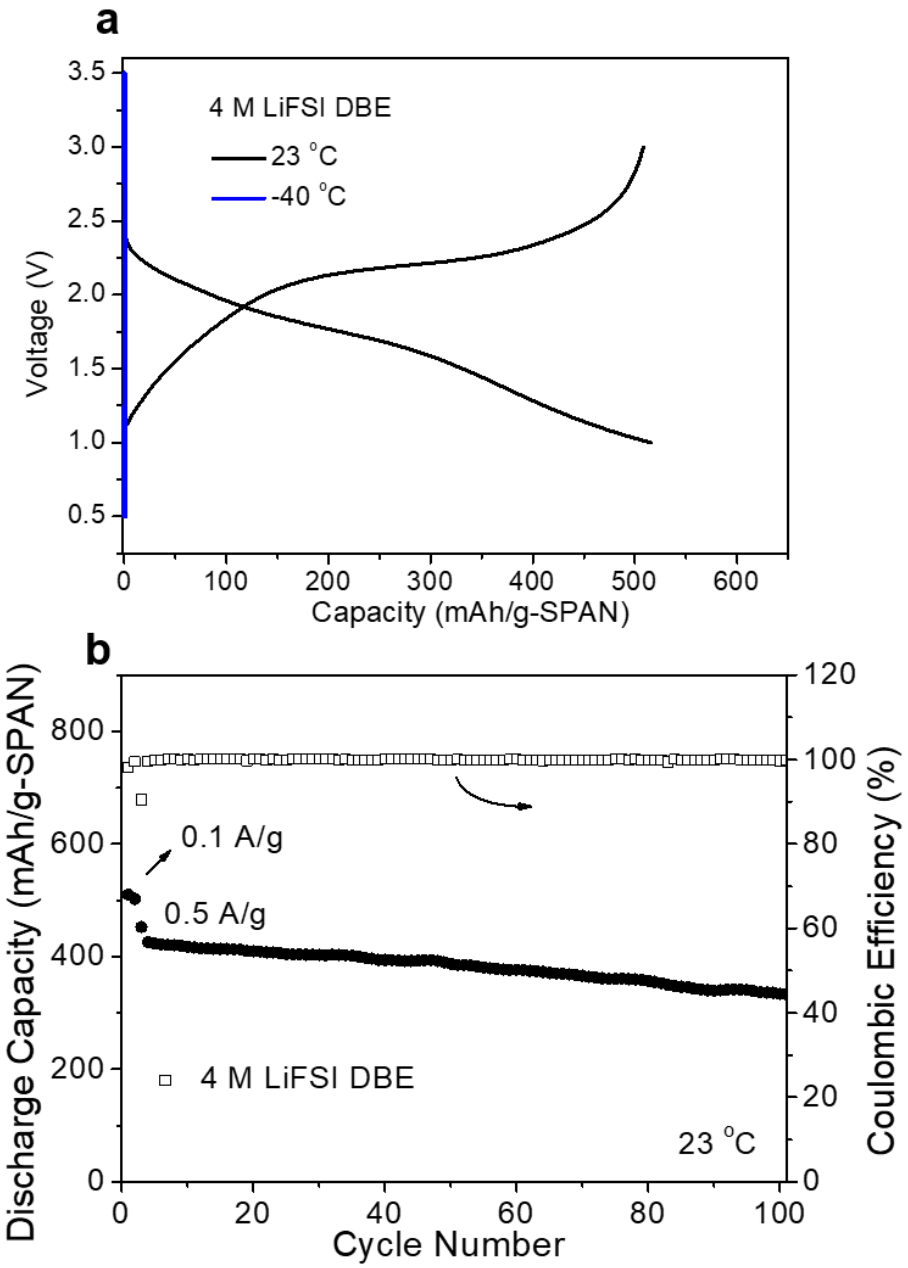

Fig. S17. (a) Voltage-capacity curves of Li//SPAN half cells in 4 M LiFSI DBE at 23 and -40 °C with a current density of 0.1 A g^{-1}. (b) Cycling performance of Li//SPAN half cells in 4 M LiFSI DBE at 23 °C and 0.5 A g^{-1}.

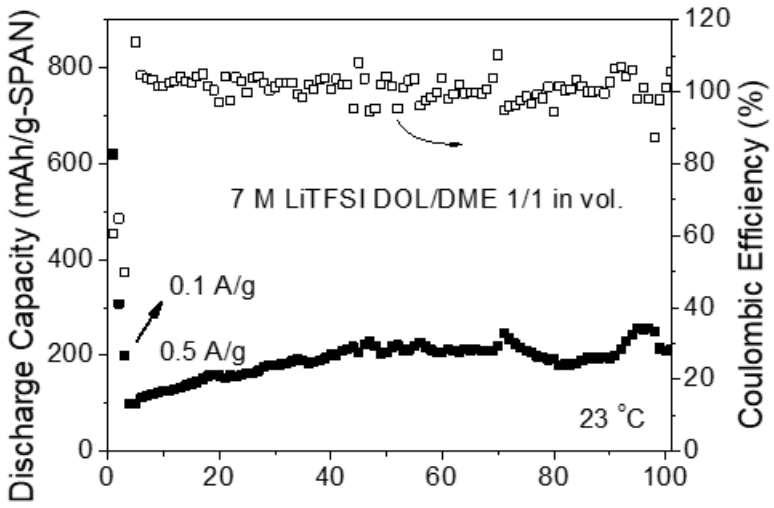

Fig. S18. Cycling performance of Li//SPAN half cells in 7 M LiTFSI DOL/DME 1/1 in vol. at 23 ^{o}C with a current density of 0.5 A g^{-1}.

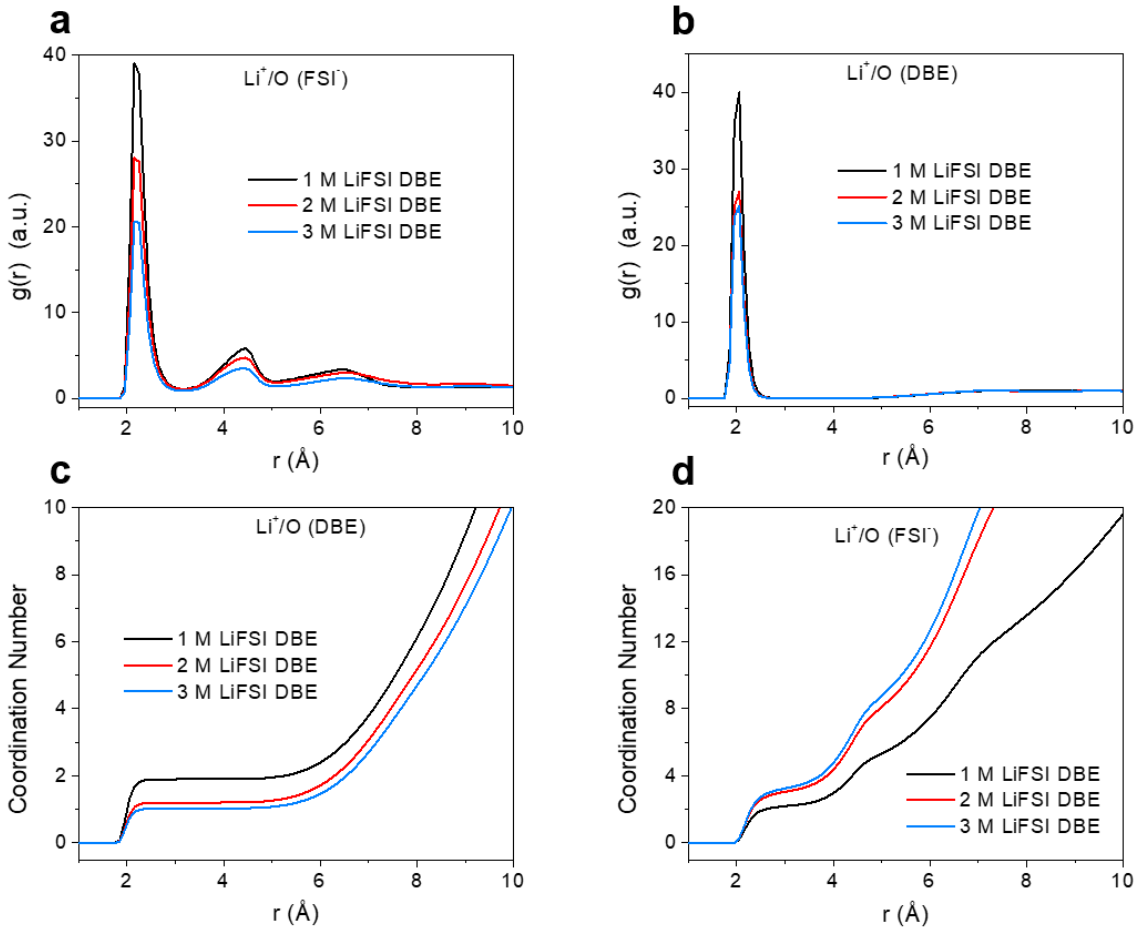

Fig. S19. Li^+ radial distribution function obtained from MD simulations of different concentration of LiFSI in DBE.

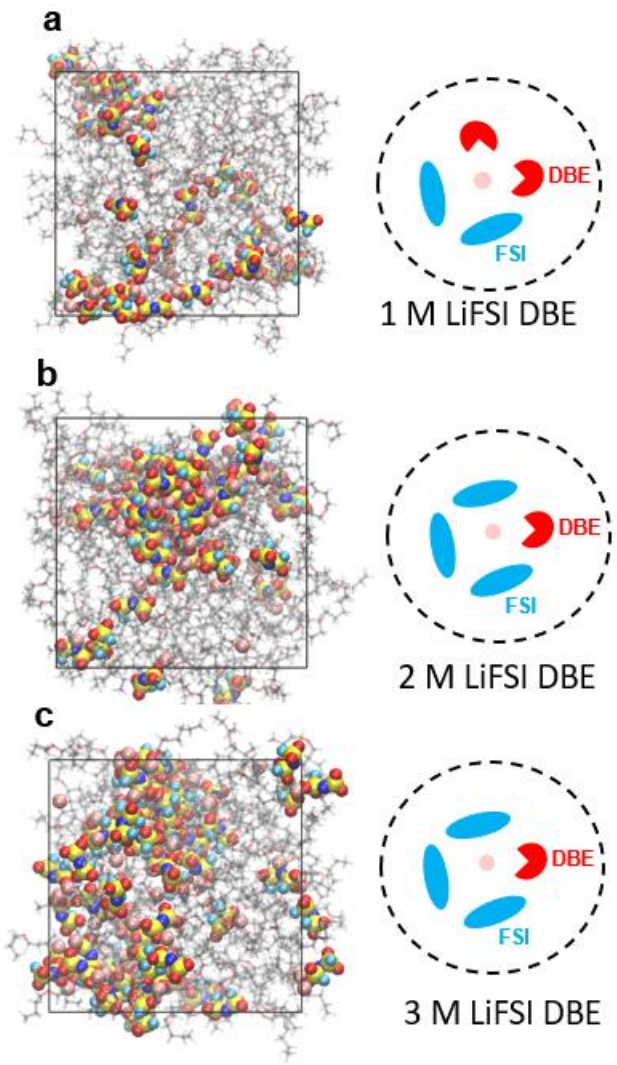

Fig. S20. (a-c) Snapshot and most representative solvation structure extracted from MD simulation of (a) 1 M LiFSI DBE, (b) 2 M LiFSI DBE, and (c) 3 M LiFSI DBE.

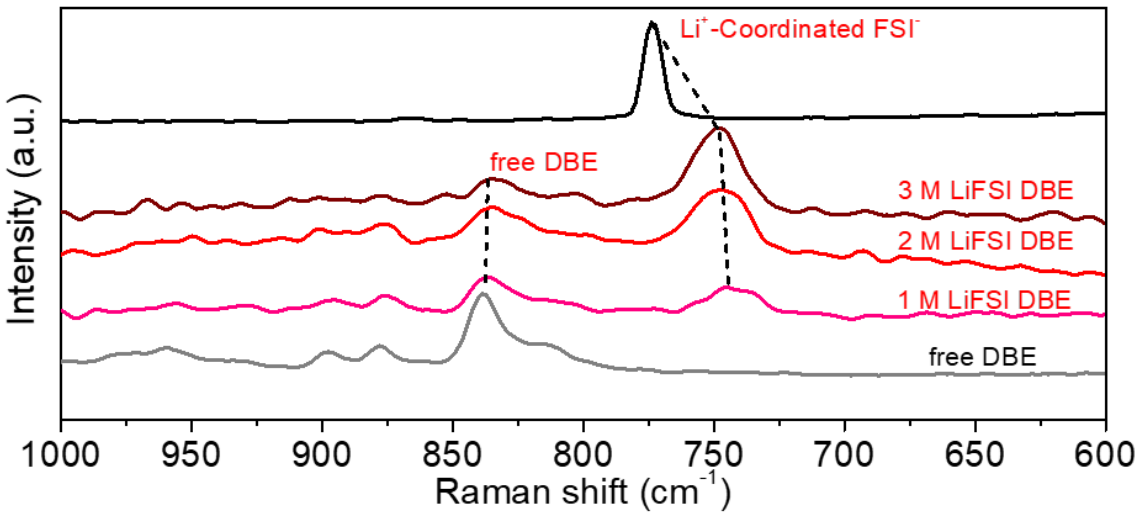

Fig. S21. Raman spectra of 1 M to 3 M LiFSI in DBE.

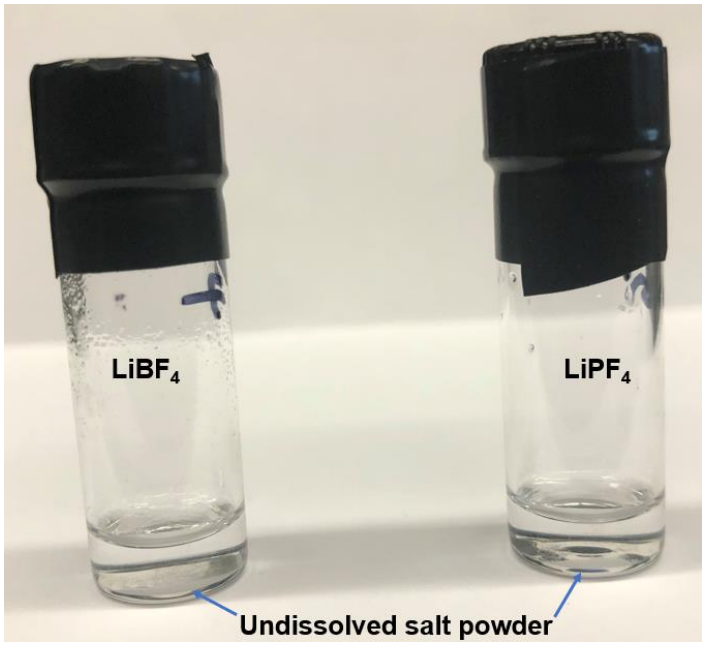

Fig. S22. Digital photographs of electrolytes prepared by the attempt of dissolving 0.1 M $LiPF_6$ and $LiBF_4$ salts in DBE. These salts were found to be insoluble in DBE even after heating at 80 ^oC overnight.

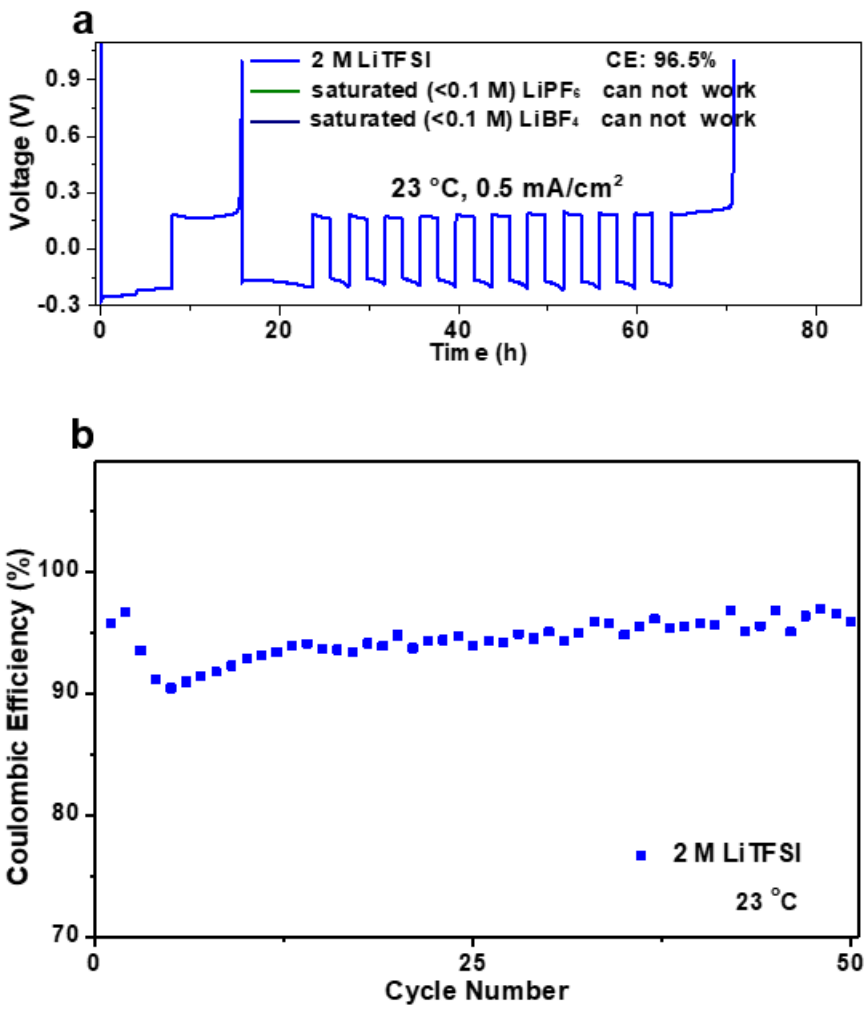

Fig. S23. (a) CE determined curves of DBE-based electrolytes with selected Li salts. (b) Long-term cycling testing of Li//Cu cells with 2 M LiTFSI DBE at 0.5 mA cm^{-2}, 1 mAh cm^{-2} and 23 °C. The supernate of the supersaturated $LiPF_6$ and $LiBF_4$ electrolytes prepared by the attempt of dissolving 0.1 M salts in DBE was used to evaluate corresponding Li//Cu cell performance. However, these cells failed to run.

Movie S1. The volatility test of DEE and DBE solvents under ambient conditions.

Movie S2. The thermal stability test of pouch cells employing DEE and DBE electrolyte systems upon exposure to 80 ^{o}C hotplate.